Blood Flow in the Human Circulatory System

Daniel Henderson

Michigan Technological University

November 26, 2025

Hemodynamics studies blood's motion, herein, we report mathematical models describing the kinematics of blood in the human macrocirculatory system. We review physiological, rheological, and mathematical foundations necessary for modeling blood flow in large vessels. We discuss numerical methods for solving the governing equations of blood flow, the incompressible Navier-Stokes equations. Finally, we present recent advances in computational hemodynamics, including physics-informed neural networks (PINN's) and fluid-structure interaction (FSI) models. (TODO)

Keywords: *computational hemodynamics, physics-informed neural networks, Deep-Riesz, discontinuous Galerkin, Lax–Wendroff, fluid–structure interaction (FSI)*

summarize final contributions here and update keywords

Taging conventions are as follows:

- Red Text means check accuracy (or clarity)
- Blue Text means not necessary
- Green Text means TODO

Work in Progress (WIP). Tips to keep in mind:
- Start w/ literature suvery, summarizing each articles contribution once. (i.e., limit repeat citation refs.), then prioritize sections by technicality
- Tag material by relevance, e.g., foundational. vs. tangential vs. speculative.
- Comparative analsyis contrasting results, models, or point out contradictions across papers
- Always consist in notation: Actively managing acroynms, abrevs., notation, and preliminaries.
- Look into [Zotero] to manage refs.

Contents

0.1 Acroynms and Abbreviations

a.e.	almost everywhere
e.g.	"exempli gratia" (for example)
i.e.	"id est" (that means)
s.s.	sufficiently smooth
s.t.	such that
r.t.	refers to
w.r.t.	with respect to
m.b.s.	must be shown
i.m.b.s.	it must be shown
i.r.t.s.	it remains to show
w.a.t.s.	we aim to show
bpm	beats per minute
wlog	without loss of generality
ODE	Ordinary Differential Equation
PDE	Partial Differential Equation
PDES	System of Partial Differential Equations
IC	Initial Condition
BC	Boundary Condition
0D	Zero dimensional
1D	One dimensional
2D	Two dimensional
3D	Three dimensional
FSI	Fluid-Structure Interaction
SB	Stenotic Blockage
RBC	Red Blood Cell
CVD	Cardiovascular disease & CVDs r.t. such diseases

0.2 Mathematical Notation

$\therefore$	consequently
$\because$	because
$\implies$	implies
$\iff$	if and only if
$:=$	defines
$\equiv$	equivalence
$\mathbb{R}$	real numbers
$\mathbb{R}^+$	positive real numbers
$\mathbb{R}^-$	negative real numbers
$\mathbb{R}^n$	n-dimensional real vector space
$\mathbb{N}$	natural numbers
$\{\boldsymbol{v_1}, \ldots, \boldsymbol{v_n}\}$	general basis of $\mathbb{R}^n$
$\{\boldsymbol{e_1}, \ldots, \boldsymbol{e_n}\}$	standard basis of $\mathbb{R}^n$
$[n] \subset \mathbb{N}$	set $\{1, 2, \ldots, n\}$
$\Omega \subset \mathbb{R}^n$	bounded domain
$\overline{\Omega}$	the closure of Ω
$\partial\Omega$	the boundary of Ω
$C^k(\Omega)$	k times continuously differentiable functions in Ω
$C_0^k(\Omega)$	k times continuously differentiable functions with compact support in Ω
$C_0^k(\overline{\Omega})$	k times continuously differentiable functions which have bounded and uniformly conti derivatives up to order k with compact support in Ω
$C_0^\infty(\Omega)$	smooth functions with compact support in Ω
$L^p(\Omega)$	Lebesgue space of p-integrable functions on Ω

Locally integrable, lipshitz, Holder continuous, Sobolev spaces, weak derivatives, distributions, test functions, multi-index notation

$d\boldsymbol{x}$	Lebesgue measure on $\mathbb{R}^n$
$dS_{\boldsymbol{x}}$	surface measure on $\partial\Omega \subset \mathbb{R}^n$
dV	volume measure on domain $\Omega \subset \mathbb{R}^3$
dS	surface measure on boundary $\partial\Omega \subset \mathbb{R}^3$
∇	gradient operator
$\Delta = \nabla^2 = \nabla \cdot \nabla(\cdot)$	Laplace operator
div	divergence of a vector field
div	divergence of a tensor field
$\boldsymbol{v}_i$	i-th component of vector $\boldsymbol{v}$
$\langle \cdot,\ \cdot \rangle_X$	inner product on vector space X
$\langle \boldsymbol{u},\ \boldsymbol{v} \rangle \equiv \langle \boldsymbol{u},\ \boldsymbol{v} \rangle_{\mathbb{R}^n}$	inner product of vectors $\boldsymbol{u}, \boldsymbol{v} \in \mathbb{R}^n$
$\partial_{\hat{\boldsymbol{n}}} = \langle \nabla,\ \hat{\boldsymbol{n}} \rangle$	normal derivative on $\partial\Omega$
$\| \cdot \|$	L^2-norm

0.3 Domain Specific Notation

R	radius of vessel with diameter $2R$
η	dynamic viscosity $\quad \left[\ Pa \cdot s\ \right]$
μ	kinematic viscosity $\quad \left[\ \frac{cm^2}{s}\ \right]$
τ	shear stress
$\dot{\gamma}$	shear rate
ρ	density field $\quad \left[\ \frac{kg}{cm^3}\ \right]$
p	pressure field
$\boldsymbol{u}$	velocity field $\quad \left[\ \frac{cm}{s}\ \right]$
W_0	Womersley number $\quad \left[\ -\ \right]$
Re	Reynolds number $\quad \left[\ -\ \right]$
Pe	Péclet number $\quad \left[\ -\ \right]$
c	concentration of a material element
D	diffusion coefficient $\quad \left[\ \frac{cm^2}{s}\ \right]$
t	time $\quad \left[\ s\ \right]$
T	terminal time $\quad \left[\ s\ \right], t > 0$
ω	angular frequency $\quad \left[\ \frac{rad}{s}\ \right]$
$\boldsymbol{f_b}$	body force per unit volume $\quad \left[\ \frac{N}{cm^3}\ \right]$

0.4 Mathematical Foundations

Assume Zermelo-Fraenkel set theory with the axiom of choice (ZFC), and according to Cohen, it's consistent if we take the continuum hypothesis (CH); a necessary posulate in continuum mechanics. A *domain* r.t. an open and bounded subset of $\mathbb{R}^n$ with nonempty interior Ω°, for $N \in [3]$. By the Heine-Borel theorem, every domain Ω has a well-defined boundary $\partial\Omega$ with compact closure $\overline{\Omega} = \Omega \cup \partial\Omega$. The compact domains of $\mathbb{R}^N$ are precisely the closed and bounded subsets of $\mathbb{R}^N$. When every path between two points in Ω may be continously contrated to a point without leaving Ω, we say that Ω is *simply connected*.

Given domain Ω, the function sp. $\mathcal{F}(\Omega)$ is the vector sp. $(F(\Omega), K)$ of scalar valued functions $f : \Omega \to K$. E.g. $C^0(\Omega)$ r.t. $(C(\Omega), \mathbb{R})$ all continuous real valued functions on Ω. Let sp. $C^k(\Omega)$ be the continuous and k-times continuously differentiable functions on Ω, then $C^k(\overline{\Omega})$ r.t. $f \in C^k(\Omega)$ s.t f and it's derivatives up to order k may be continuously extended to the boundary $\partial\Omega$. The sp. $C^\infty(\Omega)$ is the intersection of all $C^k(\Omega)$ for $k \geq 0$, i.e. the infinitely differentiable functions on Ω. And $C^k(\Omega;\ \mathbb{R}^m)$ denotes the functions $\boldsymbol{f} : \Omega \to \mathbb{R}^m$ with components in $C^k(\Omega)$, i.e., $\boldsymbol{f} = (f_i)_{i\in[m]}$ with $f_i \in C^k(\Omega)$ for all $i \in [m]$.

Let $n = \dim(\Omega)$, then we say

$\phi : \Omega \to \mathbb{R}$ r.t. a *scalar field*,

$\boldsymbol{f} : \Omega \to \mathbb{R}^n$ r.t. a *vector field*,

$\boldsymbol{T} : \Omega \to \mathbb{R}^{n\times n}$ r.t. a *(second-order) tensor field*,

and we write $\phi(\boldsymbol{x})$, $\boldsymbol{f}(\boldsymbol{x})$, and $\boldsymbol{T}(\boldsymbol{x})$[1] for the values at a point $\boldsymbol{x} \in \Omega$. When refering to a physical quantity, it's measurement units are indicated as $[\ \cdot\ ]$; whereas dimensionless quantities are indicated as $[\ -\ ]$. The k-th partial derivative of ϕ w.r.t. coordinate x_i is

$$\partial^k_{x_i}\phi \ \equiv\ \frac{\partial^k \phi}{\partial x_i^k}.$$

The generalized derivative of order $|\alpha|$ of scalar field ϕ is

$$D^\alpha\phi \ \equiv\ \frac{\partial^{|\alpha|}\phi}{\partial x_1^{\alpha_1}\,\partial x_2^{\alpha_2}\,\ldots\,\partial x_n^{\alpha_n}},$$

where $\alpha = (\alpha_1, \alpha_2, \ldots, \alpha_n)$ is a multi-index with $|\alpha| = \alpha_1 + \alpha_2 + \ldots + \alpha_n$. For $|\alpha| = 1$, $D^\alpha\phi$ is a first-order partial derivative of ϕ, e.g. $\partial_{x_i}\phi$ where $\alpha_i = 1$ and $\alpha_j = 0\ \forall j \in [n]\ :\ j \neq i$.

reserve multi-index notation for later when we work with weak derivatives, distributions, Sobolev

For real-valued $\phi \in C^1(\Omega)$, the partial derivative w.r.t. coordinate x_i is

$$\partial_{x_i}\phi = \frac{\partial\phi}{\partial x_i}.$$

[1] Note, for tensor $\boldsymbol{T}(\boldsymbol{x}) \in \mathbb{R}^{n\times n}$, $\exists$ a linear map $A : \mathbb{R}^n \to \mathbb{R}^n$ s.t. $\boldsymbol{T}(\boldsymbol{x})(\boldsymbol{u}) \mapsto A\,\boldsymbol{u}$ for all $\boldsymbol{u} \in \mathbb{R}^n$.

In coordinate-free notation, for $\boldsymbol{x} \in \Omega$ and $\hat{\boldsymbol{n}} \in \mathbb{R}^n$, the normal derivative is

define as declared in notation sec

$$\partial_{\hat{\boldsymbol{n}}}\phi(\boldsymbol{x}) \;:=\; \langle \nabla\phi(\boldsymbol{x}),\; \hat{\boldsymbol{n}} \rangle_{\mathbb{R}^n}.$$

For Lebesgue measure $d\boldsymbol{x}$ on $\mathbb{R}^n$ the integral of ϕ in Ω is

$$\int_\Omega \phi(\boldsymbol{x})\, d\boldsymbol{x}.$$

If $\partial\Omega \in C^1$, then $\phi \in C^1(\overline{\Omega}) \supset L^1(\partial\Omega)$ and the integral at the boundary is

$$\int_{\partial\Omega} \phi(\boldsymbol{x})\, dS_{\boldsymbol{x}}.$$

The gradient and Laplacian of ϕ are (respectively):

$$\begin{aligned}
\phi \;&\mapsto\; \boldsymbol{\nabla}(\phi) \;\equiv\; \nabla\phi \;=\; \left(\partial_{x_1}, \ldots, \partial_{x_N}\right)^\top \;=\; (\partial_{x_i}\phi)_{\forall i[n]}\,. \\
\phi \;&\mapsto\; \Delta\phi \;\equiv\; \nabla\cdot\nabla\phi \;=\; \sum_{\forall i[n]} \partial^2_{x_i}\phi.
\end{aligned}$$

For vector-valued $\boldsymbol{f} \in C^1(\Omega;\mathbb{R}^n)$ with components $\boldsymbol{f} = (f_i)_{\forall i\in[n]}$, the divergence is

$$\operatorname{div}\boldsymbol{f} \;:=\; \nabla\cdot\boldsymbol{f} \;=\; \sum_{\forall i\in[n]} \partial_{x_i} f_i \;=\; \langle \boldsymbol{f},\; \nabla\rangle_{\mathbb{R}^n}$$

The Laplacian and domain integral of $\boldsymbol{f}$ are defined component-wise:

$$\begin{aligned}
\boldsymbol{f} \;&\mapsto\; \Delta\,\boldsymbol{f} \;:=\; (\Delta f_i)_{\forall i\in[n]} \\
\boldsymbol{f} \;&\mapsto\; \int_\Omega \boldsymbol{f} \;:=\; \left(\int_\Omega f_i\, d\boldsymbol{x}\right)_{\forall i\in[n]}.
\end{aligned}$$

For tensor-valued $\boldsymbol{T} \in C^1(\Omega;\mathbb{R}^{n\times n})$ with entries $\boldsymbol{T} = (T_{ij})_{i,j=1}^n$, the divergence operator is

$$\begin{aligned}
\mathbf{div}\,\boldsymbol{T} \;&:=\; (\operatorname{div}\boldsymbol{t}_i)_{\forall i\in[n]} \;:\; \boldsymbol{t}_i \text{ is the ith row of } \boldsymbol{T} \\
&=\; (\nabla\cdot\boldsymbol{t}_i)_{\forall i\in[n]} \\
&=\; \left(\sum_{\forall j\in[n]} \partial_{x_j} T_{ij}\right)_{\forall i\in[n]} \\
&=\; (\langle \boldsymbol{t}_i,\; \nabla\rangle_{\mathbb{R}^n})_{\forall i\in[n]}\,.
\end{aligned}$$

The Laplacian and domain integral of $\boldsymbol{T}$ are again defined component-wise:

$$\Delta \boldsymbol{T} \;:=\; (\Delta T_{ij})_{\forall i,j\in[n]} \quad \text{and} \quad \int_\Omega \boldsymbol{T} \;:=\; \left(\int_\Omega T_{ij}\, d\boldsymbol{x}\right)_{\forall i,j\in[n]}.$$

Let K be compact (e.g. $\overline{\Omega}$), then the sp. $(C^k(K), \mathbb{R})$ is complete with norm

$$\|\phi\|_{C^k(K)} \;:=\; \sum_{\forall|\alpha|\in[k]} \sup_{\boldsymbol{x}\in K} |D^\alpha \phi(\boldsymbol{x})|\,.$$

meaning that every Cauchy sequence $\{\phi_j\}_{\forall j\in\mathbb{N}} \subset C^k(K)$ converges to a limit in $C^k(K)$. So the complete normed sp. $(C^k(K), \|\cdot\|_{C^k(K)})$ is banach, by the definition of banach sp. In particular, for $k=0$, we have

$$\|\phi\|_{C(\overline{\Omega})} \;:=\; \sup_{\boldsymbol{x}\in\overline{\Omega}} |\phi(\boldsymbol{x})| \;\equiv\; \max_{\boldsymbol{x}\in\overline{\Omega}} |\phi(\boldsymbol{x})| \;=\; \|\phi\|_\infty \quad (\text{since } \overline{\Omega} \text{ is compact}).$$

Let $\phi \in L^p(\Omega)$ be a real-valued measurable function on Ω, then the Lebesgue sp. $L^p(\Omega)$ is defined as

$$L^p(\Omega) \;:=\; \left\{\phi : \Omega \to \mathbb{R} \;\middle|\; \|\phi\|_{L^p(\Omega)} < \infty\right\} \quad \text{s.t.} \quad \|\cdot\|_{L^p(\Omega)} : \phi \mapsto \left(\int_\Omega |\phi(\boldsymbol{x})|^p\, d\boldsymbol{x}\right)^{1/p} \quad 1 \le p < \infty.$$

For $p=\infty$, the sp. $L^\infty(\Omega)$ is defined as

$$L^\infty(\Omega) \;:=\; \left\{\phi : \Omega \to \mathbb{R} \;\middle|\; \|\phi\|_{L^\infty(\Omega)} < \infty\right\} \quad \text{s.t.} \quad \|\cdot\|_{L^\infty(\Omega)} : \phi \mapsto \sup_{\boldsymbol{x}\in\Omega} |\phi(\boldsymbol{x})|.$$

where sup here r.t. the essential supremum. It follows that $\boldsymbol{f} \in L^p(\Omega;\ \mathbb{R}^m)$ denotes the functions whose components are in $L^p(\Omega)$, i.e., $\boldsymbol{f} = (f_i)_{i\in[m]}$ with $f_i \in L^p(\Omega)$ for all $i \in [m]$. The sp $(L^p(\Omega), \|\cdot\|_{L^p(\Omega)})$ is complete, hence a banach sp. for all $1 \le p \le \infty$.

TODO:

- forgoe until we work with a Lipschitz boundary: Hölder spaces, then Hilbert and Sobolev spaces. defs and notation, then trace thm., Poincare inequality, Rellich-Kondrachov comp. thm., etc. Distributional derivatives, test functions, multi-index notation, weak derivatives, weak formulation, etc.
- Add def. and notation for Lipschitz continuous functions/sp., $Lip(\Omega)$ and it's norm.
- Add relation of $Lip(\Omega)$ to $C^0(\Omega)$, brenner's book. Don't state why, just cite.

Work In Progress (WIP): Misc items.

- Write cylindrical operators
- Write material on directional derivatives and gradients
- Write material on Jacobian and Hessian matrices
- More detail on integration? Fubini's thm., change of variables, etc.
- Scaling argument for completeness of $C^k(K)$ sp. norm and nondimensionalization
- Define metric sp, normed sp., inner-product sp. defs and notation; include stmt. that norm's induce metrics, metrics induce norms.
- Finite dim sp.s are complete, hence banach, and hilbert under a particular choice of inner-product; state such inner-product for their sp.s.

1 Introduction

Hemodynamics studies the kinematics of blood. Our interest is the kinematic motion of blood within the human macrocirculatory system, i.e. the flow of blood in large vessels such as arteries and veins. Blood is observed as a complex fluid of formed elements suspended in plasma, thus, the rheological behavior of blood is non-trivial. We report techniques and methodologies for modeling blood's motion in large vessels.

Our report is organized as follows.

After stating our report's motivation, Sec. 1.1 provides a brief physiological review of the human circulatory system. Then Sec. 1.2 reviews the continuum hypothesis, a necessary postulate in fluid mechanics which treats blood as a continuous medium. This framing reduces the hemodynamic problem to describing blood's motion in a continuum. Then Sec. **??** discusses rheological assumptions that lead to constitutive relations between the material properties of blood. By conservation, the kinematic-viscosity Navier–Stokes (NS) equations are obtained (Sec. 1.4). The NS equations are a system of coupled nonlinear partial differential equations (PDEs), the foundation of our hemodynamic models.

Motivation The World Health Organization (WHO) claims cardiovascular diseases (CVDs) resulted in $\approx$ 32% of all deaths in 2022, the leading cause of death globally, where $\approx$ 85% of the deaths where from heart attack or stroke. In such cases the underlying CVD is often coronary artery stenosis (CAS), the narrowing of a coranary vessel due to the buildup of plaque. Such plaque is r.t. as a stenotic blockage. There is a need for evidience-based tools to predict and assess the severity of SBs, as often predicition of CAS doesn't mean an obstruction [[2]] and severity assesments often use a simple 0D lummped-parameter model. Cardiological interventionists need better tools for predicting and treating CAS.

Current clinical methods for assessing the severity of a SB rely on imaging techniques such as angiography, intravascular ultrasound (IVUS), and optical coherence tomography (OCT) to visualize the arteries and identify areas of narrowing. Such methods provide valuable information about the anatomy of the arteries, but they do not provide direct information about the functional significance of the CAS. Functional assessment of CAS typically involves measuring the fractional flow reserve (FFR), which is the ratio of the blood pressure downstream of the stenosis to the blood pressure upstream of the stenosis during maximum blood flow. However, measuring FFR requires the use of a pressure wire, which can be invasive and carries some risks. Therefore, there is a need for non-invasive methods to assess the functional significance of CAS.

cleanup, add refs

1.1 Physiology

The circulatory system is the human heart, vascular network, lungs, and organs. The systems source is the heart, transporting oxygen-rich blood to the organs and deoxygenated (and carbon dioxide-enriched) blood back to the lungs. Lungs discharge CO_2 and enrich the blood with Oxygen, referred to as the *pulmonary*

circulation and the *systemic circulation* (resp.). The *macrocirculatory system* consists of the heart and the large vessels in the systemic circulation. The arteries of the macrocirculatory system transport oxygenated blood from the heart, driving the return of deoxygenated blood in large vessels back to the heart.

A single beat of the heart propels blood through the macrocirculatory system, the "lub-dub" sound. The beat and the following sequence of events following until the successive beat is known as the *cardiac cycle*. The cardiac cycle consists of two main phases: systole and diastole, during which the heart chamber is accumulating blood and releasing blood (resp.). Normal resting heart rate is considered to be $\omega = 70$ bpm, so the cardiac cycle is approximately $0.86s$. and consists of:

1. Systole (ventricular contraction) ≈ 0.3 seconds.
2. Diastole (ventricular relaxation) ≈ 0.7 seconds.

During ventricular contraction, blood is ejected from the left ventricle into the aorta, creating a pressure wave that propagates through the arterial network. The Womersley number W_0 characterizes the pulse waves in large vessels by comparing the pulse frequency ω to the viscous effects determined by the kinematic viscosity $\mu := \eta/\rho \ \left[\ \frac{cm^2}{s} \ \right]$:

$$W_0 := \sqrt{\frac{\rho\omega U}{\eta U L^{-}2}} = \sqrt{L^2 \cdot \frac{\omega}{\mu}} \ \left[\ - \ \right] \quad \text{s.t.} \quad \begin{cases} L: \text{ characteristic length scale } \left[\ cm \ \right] \\ U: \text{ characteristic velocity scale } \left[\ \frac{cm}{s} \ \right] \\ \eta: \text{ dynamic viscosity } \left[\ Pa \cdot s \ \right] \\ \rho: \text{ blood density } \left[\ \frac{kg}{cm^3} \ \right] \end{cases}$$

High W_0 indicates large, rapid pulses where inertial effects dominate viscous effects while low W_0 indicates small, slow pulses where viscous effects dominate inertial effects. The Reynolds number Re characterizes flow in blood vessel

$$Re := L \cdot \frac{\rho U}{\eta} \ \left[\ - \ \right].$$

Low Re indicates laminar flow while high Re suggests turbulent flow. Note [5, Table 1.1, p. 10, §1.1] shows $W_0 \propto L$ and $Re \propto (L)^{-1}$; we observe large pulses and turbulent flow in large vessels and small pulses and laminar flow in small vessels. Note, most often we set $L = 2R$ where R is the radius of the vessel.

Observed Cardiac Cycle Characteristics

The blood volume of a human is approximately 5.7-6.0 liters of blood, flowing a full cycle roughly every minute. The energy driving the flow comes from oxygen and nutrients absorbed from food, creating waste products that must be removed; the *coronary artery*'s responsibility. The buildup of waste products results

in Arteriosclerosis, a narrowing of the coronary artery. leading to reduced and turbulent blood flow. (Add citations here of turbulence in the presence of stenotic arteries).

Is there a relationship between W_0 and Re we can exploit to simplify our models? Appears so...

Constituents and hematocrit. Blood consists of plasma and formed elements which we call cells. Red blood cells (RBCs) comprise $\approx 97\%$ of the cellular volume, and cellular volume is approximately $\approx 45\%$ of the blood volume. The remaining $\approx 55\%$ of blood volume is plasma, which is $\approx 90\%$ water. The ratio of RBC volume to total blood volume is the *hematocrit value* H, a key metric governing apparent viscosity η: as H increases, η typically increases (cf. S6.5.1 [4]). The formed elements suspended in plasma include white blood cells (WBCs) and platelets.

1.2 Continuum of Blood

W.a.t. simulate blood flow in a time-dependent fluid domain $\Omega_B \subset \mathbb{R}^{N+1}$; we'll take $N \equiv 3$, the natural setting for the derivations that follow. For each $t \in I_T := [0,T] \subset \mathbb{R}$, with $T > 0$, we define the fluid domain

$$\Omega_B(t) := \{\boldsymbol{x} \in \mathbb{R}^N : \boldsymbol{x} \text{ lies inside the vessel at time } t\}.$$

Formally, the fluid region is a time-dependent family of open sets $\{\Omega_B(t)\}_{\forall t \in I_T} \subset \mathbb{R}^N$ occupied by blood at time t. Let $\Omega_B(0)$ denote the *reference* configuration and $\Omega_B(t)$ the *current* configuration at time t. The fluid's computational domain refers to all possible configurations of $\Omega_B(t)$, i.e., the union over time of the spatial domains $\Omega_B(t)$, which we define by

$$\Omega_B := \{(t, \boldsymbol{x}) \ : \ t \in I_T, \boldsymbol{x} \in \Omega_B(t)\} \subset I_T \times \mathbb{R}^N.$$

For each material particle initially at $\boldsymbol{\xi} \in \Omega_B(0)$, we assume that its motion is governed by an Eulerian velocity field $\boldsymbol{u} : \Omega_B \to \mathbb{R}^N$, $(t, \boldsymbol{x}) \mapsto \boldsymbol{u}(t, \boldsymbol{x})$. Our aim in Sec. 1.2.1 is to derive equations describing the evolution of $\boldsymbol{\xi}$ as it moves from the reference configuration to the current configuration under the flow induced by $\boldsymbol{u}$. Precisely, we seek a map $\mathcal{L}_t : \Omega_B(0) \to \Omega_B(t)$ that carries each particle $\boldsymbol{\xi} \in \Omega_B(0)$ to its current position $\boldsymbol{x} \in \Omega_B(t)$ at time t.

1.2.1 Blood Dynamics

For each fixed $t \in I_T$, let the *Lagrangian map* be the map from the reference configuration to the current configuration, i.e.

$$\mathcal{L}_t : \Omega_B(0) \to \Omega_B(t), \quad \boldsymbol{\xi} \mapsto \boldsymbol{x}(t, \boldsymbol{\xi})$$

where $\boldsymbol{x}(t, \boldsymbol{\xi}) = \mathcal{L}_t(\boldsymbol{\xi})$ is the particle $\boldsymbol{\xi}$'s position at time t. We assume that, for each $t \in I_T$, the map $\mathcal{L}_t : \Omega_B(0) \to \Omega_B(t)$ is a bijection, and that $(t, \boldsymbol{\xi}) \mapsto \mathcal{L}_t(\boldsymbol{\xi})$ is sufficiently smooth in t (e.g., C^1) so that $\partial_t \boldsymbol{x}(t, \boldsymbol{\xi})$ is well-defined. The pairs $(t, \boldsymbol{x})$ and $(t, \boldsymbol{\xi})$ are respectively referred to as the Eulerian and Lagrangian coordinates. For fixed $\boldsymbol{\xi} \in \Omega_B(0)$, we sometimes write $\boldsymbol{x}(t; \boldsymbol{\xi})$ to emphasize the flow map of $\boldsymbol{\xi}$, with corresponding trajectory $T_{\boldsymbol{\xi}} = \{(t, \boldsymbol{x}(t; \boldsymbol{\xi})) \ : \ t \in I_T\}$.

Remark 1.2.1 (Eulerian vs. Lagrangian). Informally, the Eulerian description focuses on what happens at a fixed spatial location $\boldsymbol{x} \in \Omega_B(t)$ at a given time t; fields such as $\phi(t, \boldsymbol{x})$ or $\boldsymbol{u}(t, \boldsymbol{x})$ are viewed as functions of $(t, \boldsymbol{x})$. In contrast, the Lagrangian description follows individual material particles $\boldsymbol{\xi} \in \Omega_B(0)$ along their trajectories $t \mapsto \boldsymbol{x}(t; \boldsymbol{\xi})$.
Let

$$\mathrm{id}_{I_T} \times \mathcal{L}_t : I_T \times \Omega_B(0) \to \Omega_B, \quad (t, \boldsymbol{\xi}) \mapsto (t, \mathcal{L}_t(\boldsymbol{\xi})).$$

Then (where defined) its inverse is

$$\mathrm{id}_{I_T} \times \mathcal{L}_t^{-1} : \Omega_B \to I_T \times \Omega_B(0), \quad (t, \boldsymbol{x}) \mapsto (t, \mathcal{L}_t^{-1}(\boldsymbol{x})).$$

We define the Lagrangian velocity field by

$$\widehat{\boldsymbol{u}}(t, \boldsymbol{\xi}) \ := \ \partial_t \boldsymbol{x}(t, \boldsymbol{\xi}) \quad \forall (t, \boldsymbol{\xi}) \in I_T \times \Omega_B(0).$$

A change of coordinates in $\widehat{\boldsymbol{u}}$ yields the velocity field $\boldsymbol{u}$ in the Eulerian frame, i.e.,

$$\begin{aligned} \boldsymbol{u}(t, \boldsymbol{x}) \ &= \ \big(\widehat{\boldsymbol{u}} \circ (\mathrm{id}_{I_T} \times \mathcal{L}_t^{-1})\big)(t, \boldsymbol{x}). \\ &= \ \widehat{\boldsymbol{u}}\big(t, \mathcal{L}_t^{-1}(\boldsymbol{x})\big) \\ &= \ \widehat{\boldsymbol{u}}\big(t, \boldsymbol{\xi}\big) \quad \text{s.t. } \boldsymbol{\xi} \ = \ \mathcal{L}_t^{-1}(\boldsymbol{x}) \quad \forall (t, \boldsymbol{x}) \in \Omega_B. \end{aligned}$$

If $\widehat{\boldsymbol{u}}$ and $\Omega_B(0)$ are known, we arrive at the Cauchy problem for a particle trajectory in the Lagrangian

frame:

$$\begin{cases} \partial_t \boldsymbol{x}(t,\boldsymbol{\xi}) \;=\; \widehat{\boldsymbol{u}}(t,\boldsymbol{\xi}), t \in I_T, \\ \boldsymbol{x}(0,\boldsymbol{\xi}) \;=\; \boldsymbol{\xi}. \end{cases}$$

Equivalently, if $\boldsymbol{u}$ and Ω_B are known, we arrive at the Cauchy problem for a particle trajectory in the Eulerian frame:

$$\begin{cases} \dfrac{d}{dt}\,\boldsymbol{x}(t;\boldsymbol{\xi}) \;=\; \boldsymbol{u}\big(t,\boldsymbol{x}(t;\boldsymbol{\xi})\big), t \in I_T, \\ \boldsymbol{x}(0;\boldsymbol{\xi}) \;=\; \boldsymbol{\xi}. \end{cases}$$

In other words, for each $\boldsymbol{\xi} \in \Omega_B(0)$, the trajectory $t \mapsto \boldsymbol{x}(t;\boldsymbol{\xi})$ is an integral curve of the Eulerian velocity field $\boldsymbol{u}$.

Theorem 1.2.2 (Well-posedness of particle trajectories (Hadamard))**.** *TODO: State and prove well-posedness in the sense of Hadamard (solution depends Lipschitz-continuously on initial data.)*

Definition 1.2.3. Let $\phi \in C^k(\Omega_B)$ and $\widehat{\phi} \;:=\; \phi \circ \mathcal{L}_t$ so that $\widehat{\phi}(t,\boldsymbol{\xi}) \;=\; \phi(t,\boldsymbol{x}(t,\boldsymbol{\xi}))$, then the *material derivative* $D_t\phi$ is the derivative of ϕ w.r.t. t in the Lagrangian frame expressed as a function in the Eulerian frame, i.e.,

$$\begin{aligned} D_t\big(\phi(t,\boldsymbol{x})\big) \;&:=\; \partial_t\widehat{\phi}(t,\boldsymbol{\xi}), \quad \text{s.t. } \boldsymbol{\xi} \;=\; \mathcal{L}_t^{-1}(\boldsymbol{x}) \\ &=\; \frac{d}{dt}\phi(t,\boldsymbol{x}(t,\boldsymbol{\xi})), \quad \forall \boldsymbol{\xi} \in \Omega_B(0) \quad (\because\; \widehat{\phi}(t,\boldsymbol{\xi}) \;=\; \phi(t,\boldsymbol{x}(t,\boldsymbol{\xi}))). \end{aligned}$$

By the multivariable chain rule we simplify as

$$\begin{aligned} D_t\big(\phi(t,\boldsymbol{x})\big) \;&=\; \partial_t\phi(t,\boldsymbol{x}) + \nabla\phi(t,\boldsymbol{x}) \cdot \boldsymbol{u}(t,\boldsymbol{x}) \quad (\because \text{chain rule and since } \partial_t\boldsymbol{x} = \boldsymbol{u}) \\ &=\; \partial_t\phi + \langle \nabla\phi,\; \boldsymbol{u}\rangle_{\mathbb{R}^N} \quad \text{in } \Omega_B. \end{aligned}$$

By the divergence relationship $\operatorname{div}(\phi\boldsymbol{u}) \;=\; \nabla\phi \cdot \boldsymbol{u} + \phi \operatorname{div}(\boldsymbol{u})$, we rewrite as

$$D_t\big(\phi\big) \;=\; \partial_t\phi + \operatorname{div}(\phi\boldsymbol{u}) - \phi \operatorname{div}(\boldsymbol{u}) \quad \text{in } \Omega_B.$$

The material derivative 1.2.3 measures the rate of variation of ϕ along trajectory $T_{\boldsymbol{\xi}}$ expressed in the Eulerian variables. The literature also r.t. D_t as the *substantial derivative*, *advective derivative*, *lagrangian derivative*, or *convective derivative*.

Now differentiating $\widehat{\boldsymbol{u}}$ w.r.t. t yields the acceleration vector field $\widehat{\boldsymbol{a}}$ in the Lagrangian and Eulerian frame

respectively:

$$
\begin{aligned}
&\widehat{\boldsymbol{a}}(t,\boldsymbol{\xi}) \;:=\; \partial_t \widehat{\boldsymbol{u}}(t,\boldsymbol{\xi}) = \partial_t^2 \boldsymbol{x}(t,\boldsymbol{\xi}) \quad \forall \boldsymbol{\xi} \in \Omega_B(0) \\
&\iff \boldsymbol{a} \;=\; D_t \boldsymbol{u} \;=\; \partial_t \boldsymbol{u} + (\boldsymbol{u}\cdot\nabla)\boldsymbol{u} \quad \text{in } \Omega_B(t) \\
&\boldsymbol{a}(t,\boldsymbol{x}) \;=\; \partial_t \boldsymbol{u}(t,\boldsymbol{x}) + (\boldsymbol{u}(t,\boldsymbol{x})\cdot\nabla)\boldsymbol{u}(t,\boldsymbol{x}) \\
&\qquad\quad =\; \partial_t \boldsymbol{u}(t,\boldsymbol{x}) + \sum_{\forall i\in[N]} u_i(t,\boldsymbol{x})\partial_{x_i}\boldsymbol{u}(t,\boldsymbol{x}) \quad \forall (t,\boldsymbol{x}) \in I_T \times \Omega_B(t) \\
&\iff \boldsymbol{a} \;=\; \partial_t \boldsymbol{u} + \sum_{\forall i\in[N]} u_i\, \partial_{x_i}\boldsymbol{u} \\
&\qquad\quad =\; \partial_t \boldsymbol{u} + \langle \nabla,\, \boldsymbol{u}\rangle_{\mathbb{R}^N}\boldsymbol{u} \quad \text{in } \Omega_B.
\end{aligned}
$$

We denote the deformation gradient tensor in Lagrangian and Eulerian form by $\widehat{\boldsymbol{F}}_t$ and $\boldsymbol{F}_t$, respectively, defined by

$$
\begin{aligned}
&\widehat{\boldsymbol{F}}_t(\boldsymbol{\xi}) \;:=\; \nabla_{\boldsymbol{\xi}} \mathcal{L}_t(\boldsymbol{\xi}) \quad \forall \boldsymbol{\xi} \in \Omega_B(0). \\
&\qquad \iff \boldsymbol{F}_t(\boldsymbol{x}) \;=\; \nabla_{\boldsymbol{\xi}} \mathcal{L}_t(\mathcal{L}_t^{-1}(\boldsymbol{x})) \;=\; \partial_{\boldsymbol{\xi}} \boldsymbol{x}(t,\boldsymbol{\xi}) \quad \forall (t,\boldsymbol{x}) \in \Omega_B.
\end{aligned}
$$

The tensor $\boldsymbol{F}_t$ measures the spatial deformation of infinitesimal fluid elements as they move from the reference configuration to the current configuration under $\mathcal{L}_t$ along trajectory $T_{\boldsymbol{\xi}}$. Suppose for each fixed t the mapping $\mathcal{L}_t : \Omega_B(0) \to \Omega_B(t)$ is a C^1–diffeomorphism with $\det \widehat{\boldsymbol{F}}_t(\boldsymbol{\xi}) > 0 \forall \boldsymbol{\xi} \in \Omega_B(0)$[2]. Then $\widehat{\boldsymbol{F}}_t(\boldsymbol{\xi})$ is invertible, and we define:

$$
\begin{aligned}
&\widehat{J}_t(\boldsymbol{\xi}) \;:=\; \det\left(\widehat{\boldsymbol{F}}_t(\boldsymbol{\xi})\right) \quad \forall \boldsymbol{\xi} \in \Omega_B(0). \\
&\qquad \iff J_t(\boldsymbol{x}) \;=\; \det\left(\widehat{\boldsymbol{F}}_t(\mathcal{L}_t^{-1}(\boldsymbol{x}))\right) \quad \forall (t,\boldsymbol{x}) \in \Omega_B.
\end{aligned}
$$

We r.t. such measure of spatial deformation $\widehat{J}_t(\boldsymbol{\xi})$ as the Jacobian determinant of $\mathcal{L}_t$ at time t. The following lemma shows that $\partial_t J_t$ relates to the fluid's divergence $\operatorname{div}(\boldsymbol{u})$.

Lemma 1.2.4. *The Jacobian determinant $J_t(\boldsymbol{x})$ satisfies*

$$
D_t J_t(\boldsymbol{x}) \;=\; J_t(\boldsymbol{x})\, div(\boldsymbol{u}(t,\boldsymbol{x})) \quad \forall (t,\boldsymbol{x}) \in \Omega_B.
$$

Proof. Ref [3], lemma 2.1, pg. 20, for proof. □

Literature often r.t. relation in lem. 1.2.4 as the *Euler expansion formula*, or *Jacobi's equation*.

[2]Recall the $\det \widehat{\boldsymbol{F}}$ may be interpreted as the signed volume change of an infinitesimal parallelepiped spanned by the column vectors of $\widehat{\boldsymbol{F}}$; thus, $\det \widehat{\boldsymbol{F}}_t(\boldsymbol{\xi}) > 0$ ensures that the orientation of fluid elements is preserved under the mapping $\mathcal{L}_t$ at time t. Moreover, it prevents unphysical scenarios such as interpenetration of matter consisting of negative volumes.

Let $V(t)$ denote a measurable material volume at time t that moves with the fluid flow, i.e.,

$$V(t) \subset \Omega_B(t), \quad \text{for each } t \in I_T$$

Equivalently, $V(t)$ is the image of some reference volume $V(0) \subset \Omega_B(0)$ under the Lagrangian mapping $\mathcal{L}_t$, i.e.,

$$V(t) = \mathcal{L}_t\big(V(0)\big).$$

The following theorem, known as the Reynolds Transport Theorem, relates the time derivative of an integral over the material derivative of $V(t)$.

Theorem 1.2.5 (Reynolds Transport Theorem)**.** *Let $V(0) \subset \Omega_B(0)$ be a material volume in the reference configuration, and $V(t) \subset \Omega_B(t)$ its image in the current configuration under $\mathcal{L}_t$. Then for $\phi \in L^1(\Omega_B)$ we have*

$$\begin{aligned}\frac{d}{dt}\int_{V(t)} \phi(t,\boldsymbol{x})\, d\boldsymbol{x} &= \int_{V(t)} D_t\phi(t,\boldsymbol{x}) + \phi(t,\boldsymbol{x})\,\langle \nabla,\ \boldsymbol{u}(t,\boldsymbol{x})\rangle\, d\boldsymbol{x} \\ &= \int_{V(t)} \partial_t\phi(t,\boldsymbol{x}) + \langle \nabla,\ \phi(t,\boldsymbol{x})\boldsymbol{u}(t,\boldsymbol{x})\rangle\, d\boldsymbol{x}\end{aligned}$$

Proof. Observe

$$\begin{aligned}\frac{d}{dt}\int_{V(t)} \phi(t,\boldsymbol{x}) &= \frac{d}{dt}\int_{V(0)} \widehat{\phi}(t,\boldsymbol{\xi})\widehat{J}_t(\boldsymbol{\xi})\, d\boldsymbol{\xi} \quad \text{(by 1.2.3 and 1.2.4).} \\ &= \int_{V(0)} \partial_t\Big(\widehat{\phi}(t,\boldsymbol{\xi})\widehat{J}_t(\boldsymbol{\xi})\Big)\, d\boldsymbol{\xi} \\ &= \int_{V(0)} \partial_t\Big(\widehat{\phi}(t,\boldsymbol{\xi})\Big)\widehat{J}_t(\boldsymbol{\xi}) + \widehat{\phi}(t,\boldsymbol{\xi})\partial_t\Big(\widehat{J}_t(\boldsymbol{\xi})\Big)\, d\boldsymbol{\xi} \quad \text{(chain rule)} \\ &= \int_{V(t)} D_t\big(\phi(t,\boldsymbol{x})\big)\, d\boldsymbol{x} + + \int_{V(0)} \widehat{\phi}(t,\boldsymbol{\xi})\widehat{J}_t(\boldsymbol{\xi})\mathrm{div}(\boldsymbol{u}(t,x(t,\boldsymbol{\xi})))\, d\boldsymbol{\xi} \quad \text{(by again 1.2.3 and 1.2.4).} \\ &= \int_{V(t)} D_t\big(\phi(t,\boldsymbol{x})\big)\, d\boldsymbol{x} + \int_{V(t)} \phi(t,\boldsymbol{x})\mathrm{div}(\boldsymbol{u}(t,\boldsymbol{x}))\, d\boldsymbol{x} \quad \text{(change of variables)} \\ &= \int_{V(t)} \partial_t\phi(t,\boldsymbol{x}) + \langle \nabla,\ \phi(t,\boldsymbol{x})\boldsymbol{u}(t,\boldsymbol{x})\rangle\, d\boldsymbol{x} \quad \text{(by 1.2.3).}\end{aligned}$$

□

cleanup? Also, corollary by applying divergence theorem

1.3 NS-derivation

In the following derivations we let $N \equiv 3$ so that $\Omega_B(t) \subset \mathbb{R}^3$. We assume blood fluid is a continuum that deforms continuously, i.e., at every point $\boldsymbol{x} \in \Omega_B(t)$ and time $t \in I_T$, the blood's kinematic quantities are described by sufficiently smooth fields. At microscopic scales, this continuum hypothesis breaks down, since matter is a discrete collection of molecules, but at macroscopic scales empirical evidence suggests such models remain accurate.

Let blood's velocity, thermodynamic pressure, and density fields be

$$\begin{aligned}
&\boldsymbol{u} : \Omega_B \to \mathbb{R}^3,\ (t,x,y,z) \mapsto (u_1(t,x,y,z),\, u_2(t,x,y,z),\, u_3(t,x,y,z))^\top, \quad \left[\ \frac{cm}{s}\ \right] \\
&p : \Omega_B \to \mathbb{R}^+,\ (t,x,y,z) \mapsto p(t,x,y,z), \quad \left[\ \frac{N}{cm^2}\ \right] \\
&\rho : \Omega_B \to \mathbb{R}^+,\ (t,x,y,z) \mapsto \rho(t,x,y,z), \quad \left[\ \frac{kg}{cm^3}\ \right].
\end{aligned}$$

For each $t \in I_T$, herein assume $\Omega_B(t)$ is simply connected and boundary $\partial\Omega_B(t) \in C^1$, so, any closed curve in $\Omega_B(t)$ can be continuously contracted to a point within $\Omega_B(t)$; such an assumption is reasonable in a healthy vessel with a smooth wall. This regularity allows us to globally define geometric quantities such as surface differential operators on the fluids boundary $\partial\Omega_B$, then we may apply stokes theorem and Green's identities on the C^1 boundaries, useful for obtaining weak integro-differential and variational formulations.

Remark 1.3.1. A weaker regularity condition is that $\partial\Omega_B$ is Lipschitz. Here we must rely on standard trace theorems for Sobolev spaces (e.g. $H^1(\Omega_B(t))$). In particular, the outward unit normal is then defined a.e. on $\partial\Omega_B(t)$, so we can meaningfully speak of normal and tangential components of vector fields on the boundary.

Definition 1.3.2 (Incompressible fluid)**.** A fluid is *incompressible* if for each material element $V(0) \subset \Omega_B(0)$, the density of that element remains constant in time, i.e.

$$\rho\big(t, \boldsymbol{x}(t,\boldsymbol{\xi})\big) \ = \ \rho_{V(0)} \in \mathbb{R}^+, \quad \forall (t,\boldsymbol{\xi}) \in I_T \times V(0),$$

where constant $\rho_{V(0)}$ can depend on initial fluid element $V(0)$.

Definition 1.3.3 (Incompressible flow)**.** A flow is *incompressible* in Ω_B if the material derivative of the density vanishes,

$$D_t\rho = 0 \quad \text{in } \Omega_B.$$

In our model we further assume a uniform initial density, so def 1.3.2 may be written as

$$\rho_{V(0)} \ = \ \rho_0 \in \mathbb{R}^+ \quad \forall\, V(0) \subset \Omega_B(0),$$

for some constant ρ_0 independent of material element $V(0)$. Therefore uniform density in the reference configuration implies constant density along trajectory $T_{\boldsymbol{\xi}}$ to any current configuration, i.e.,

$$\begin{aligned}\rho\big(t, \boldsymbol{x}(t, \boldsymbol{\xi})\big) \;&=\; \rho_0 \in \mathbb{R}^+, \quad \forall (t, \boldsymbol{\xi}) \in I_T \times \Omega_B(0). \\ &\Longrightarrow\; \rho(t, \boldsymbol{x}) \;=\; \rho_0 \in \mathbb{R}^+, \quad \forall (t, \boldsymbol{x}) \in \Omega_B.\end{aligned}$$

Taking the material derivative yields $D_t\rho = 0$ in Ω_B – In summary, we've shown:

$$\text{Incompressibile Fluid 1.3.2} \quad \Longrightarrow \quad \text{Incompressible Flow 1.3.3.}$$

Note, the converse is not generally true: an incompressible flow ($D_t\rho = 0$) only preserves density along $T_{\boldsymbol{\xi}}$, allowing $\rho = \rho(\boldsymbol{x})$ to vary spatially in the Eulerian frame. But particularly here, uniform initial density in $\Omega_B(0)$ implies constant density in Ω_B under the assumption of incompressible flow.

Remark 1.3.4 (Divergence-free condition). Mass conservation for a fluid with density ρ and velocity $\boldsymbol{u}$ yields the continuity equation

$$\partial_t\rho + \mathrm{div}(\rho\boldsymbol{u}) = 0 \quad \Longleftrightarrow \quad D_t\rho + \rho\,\mathrm{div}\boldsymbol{u} = 0 \quad \text{in } \Omega_B.$$

For an incompressible fluid with constant density $\rho \equiv \rho_0$, Definition 1.3.2 implies $D_t\rho = 0$, so

$$0 = D_t\rho + \rho_0 \mathrm{div}\boldsymbol{u} \quad \Longrightarrow \quad \mathrm{div}\boldsymbol{u} = 0 \quad \text{in } \Omega_B.$$

Combining this with Lemma 1.2.4,

$$D_t J_t = J_t \mathrm{div}\boldsymbol{u},$$

we obtain $D_t J_t = 0$, hence $J_t(\boldsymbol{x})$ is constant along material trajectories. With the natural choice $\mathcal{L}_0 = \mathrm{Id}$ we have $J_0 \equiv 1$, so incompressible flow is equivalent to

$$J_t(\boldsymbol{x}) \equiv 1 \quad \text{and} \quad \mathrm{div}\boldsymbol{u} = 0.$$

We refer to $\nabla \cdot \boldsymbol{u} = \mathrm{div}\boldsymbol{u} = 0$ as the *divergence-free condition* in $\Omega_B(t)$.

By assumption blood is incompressible and newtonian, linear momentum balance follows from Newton's 2nd Law ($F = ma$) for an infinitesimal fluid element $V(t) \subset \Omega_B(t)$.

Definition 1.3.5. The linear momentum balance for a fluid element $V \in \Omega_B$ under flow $\boldsymbol{u}$ is

$$\frac{d}{dt}\int_{V(t)} \rho\,\boldsymbol{u}\,dV \;=\; \int_{V(t)} \mathbf{div}(\boldsymbol{T})\,dV + \int_{V(t)} \rho\,\boldsymbol{f_b}\,dV, \quad (\because\ \rho \equiv \rho_0)$$

where $\boldsymbol{T}$ is the Cauchy stress tensor describing the fluids deformation, $\boldsymbol{f_b}$ may be some body force per unit mass $\left[\ \frac{cm}{s^2}\ \right]$.

By applying the Reynolds Transport Theorem 1.2.5 to linear momentum balance 1.3.5, we obtain the integral form of linear momentum balance:

$$\int_{V(t)} \rho\, \partial_t \boldsymbol{u}\, dV + \int_{\rho V(t)} \rho\, \boldsymbol{u}\, \langle \boldsymbol{u},\ \hat{\boldsymbol{n}} \rangle\, dS \ =\ \int_{V(t)} \mathbf{div}(\boldsymbol{T})\, dV + \int_{V(t)} \rho\, \boldsymbol{f_b}\, dV,$$

for any material volume $V(t) \subset \Omega_B(t)$. By the divergence theorem, we may rewrite the surface integral as a volume integral

$$\int_{V(t)} \rho\, \partial_t \boldsymbol{u}\, dV + \int_{V(t)} \mathrm{div}(\rho\, \boldsymbol{u} \otimes \boldsymbol{u})\, dV \ =\ \int_{V(t)} \mathbf{div}(\boldsymbol{T})\, dV + \int_{V(t)} \rho\, \boldsymbol{f_b}\, dV,$$

Since $V(t)$ is arbitrary, the integrands must be equal a.e. in $\Omega_B(t)$, yielding differential form of linear momentum balance:

$$\rho\, \partial_t \boldsymbol{u} + \mathrm{div}(\rho\, \boldsymbol{u} \otimes \boldsymbol{u}) \ =\ \mathbf{div}(\boldsymbol{T}) + \rho\, \boldsymbol{f_b}, \qquad \text{in } \Omega_B(t)$$

By incompressibility assumption of blood fluid 1.3.2 we have $\rho \equiv \rho_0$ constant in $\Omega_B(t)$, so the linear momentum balance simplifies to

$$\rho\, \partial_t \boldsymbol{u} + \rho\, \mathrm{div}(\boldsymbol{u} \otimes \boldsymbol{u}) \ =\ \mathbf{div}(\boldsymbol{T}) + \rho\, \boldsymbol{f_b}, \qquad \text{in } \Omega_B(t)$$

Using the vector calculus identity $\mathrm{div}(\boldsymbol{u} \otimes \boldsymbol{u}) = (\nabla \cdot \boldsymbol{u})\, \boldsymbol{u} + (\boldsymbol{u} \cdot \nabla)\boldsymbol{u}$ we have

$$\begin{aligned} \mathrm{div}(\boldsymbol{u} \otimes \boldsymbol{u}) \ &=\ \big(\nabla \cdot \boldsymbol{u}\big)\, \boldsymbol{u} + (\boldsymbol{u} \cdot \nabla)\boldsymbol{u} \\ &=\ 0 \cdot \boldsymbol{u} + (\boldsymbol{u} \cdot \nabla)\boldsymbol{u} \quad (\because \mathrm{div}\, \boldsymbol{u} \ =\ 0 \text{ by remark 1.3.4}) \\ \implies \rho\, \partial_t \boldsymbol{u} + \rho\, (\boldsymbol{u} \cdot \nabla)\boldsymbol{u} \ &=\ \mathbf{div}(\boldsymbol{T}) + \rho\, \boldsymbol{f_b}, \qquad \text{in } \Omega_B(t) \end{aligned}$$

so the linear momentum balance 1.3.5 for incompressible fluid simplifies to the following form.

Definition 1.3.6. The differential form of linear momentum balance for an incompressible fluid element $V \in \Omega_B$ under flow $\boldsymbol{u}$ is

$$\rho(\partial_t \boldsymbol{u} + (\boldsymbol{u} \cdot \nabla)\boldsymbol{u}) \ =\ \mathbf{div}(\boldsymbol{T}) + \rho \boldsymbol{f_b}, \qquad \text{in } \Omega_B(t)$$

The linear momentum balance equation above is not closed since the Cauchy stress tensor $\boldsymbol{T}$ is unknown. To close the system, we need a constitutive law relating $\boldsymbol{T}$ to kinematic quantities such as the velocity field $\boldsymbol{u}$ and its derivatives.

Let the rate-of-deformation tensor be the symmetric part of the velocity gradient,

$$\boldsymbol{D}(\boldsymbol{u}) \;:=\; \tfrac{1}{2}\big(\nabla \boldsymbol{u} + (\nabla \boldsymbol{u})^{\top}\big)$$

Note that $\boldsymbol{u} \mapsto \boldsymbol{D}(\boldsymbol{u})$ captures spatial deformations of element V in Ω_B under flow $\boldsymbol{u}$. Here $\boldsymbol{D}(\boldsymbol{u})$ is related to the gradient deformation tensor $\boldsymbol{F}_t$ via

$$\boldsymbol{D}(\boldsymbol{u}) \;=\; \tfrac{1}{2}\, D_t \boldsymbol{F}_t\, \boldsymbol{F}_t^{-1}$$

where $D_t \boldsymbol{F}_t$ is the material derivative of $\boldsymbol{F}_t$ (see ref [3], sec. 3.4, pg. 39, for derivation).

Definition 1.3.7. A fluid is *Newtonian* if its Cauchy stress tensor $\boldsymbol{T}$ depends linearly on the rate-of-deformation tensor $\boldsymbol{D}(\boldsymbol{u})$.

Definition 1.3.8. A fluid is *isotropic* if its constitutive response is independent of the coordinate system. Writing the Cauchy stress as $\boldsymbol{T} = \boldsymbol{T}(\boldsymbol{D})$, isotropy means that for every orthogonal rotator $\boldsymbol{Q} \in \mathrm{SO}(3)$,

$$\boldsymbol{Q}\,\boldsymbol{T}(\boldsymbol{D})\,\boldsymbol{Q}^{\top} \;:=\; \boldsymbol{T}\big(\boldsymbol{Q}\,\boldsymbol{D}\,\boldsymbol{Q}^{\top}\big).$$

Where $SO(3) := \{\boldsymbol{Q} \in \mathbb{R}^{3\times 3} : \boldsymbol{Q}\,\boldsymbol{Q}^{\top} = \mathrm{I},\ \det(\boldsymbol{Q}) = 1\}$ is the special orthogonal group in $\mathbb{R}^3$.

Remark 1.3.9 (Isotropy implication). By 1.3.8, the Cauchy stress $\boldsymbol{T}$ of an isotropic fluid depends only on the invariants of $\boldsymbol{D}(\boldsymbol{u})$, i.e., the eigenvalues of $\boldsymbol{D}(\boldsymbol{u})$.

Remark 1.3.10 (Simple vs. complex fluids). In the terminology of continuum mechanics, a *simple* fluid is one whose constitutive response at a point depends only on the instantaneous values of kinematic quantities (such as the rate-of-deformation tensor $\boldsymbol{D}(\boldsymbol{u})$), and not on their past history. The Newtonian, isotropic model in Definition 1.3.12 is a prototypical simple fluid. More complex models (e.g. viscoelastic fluids) incorporate memory effects so that the stress depends on the deformation history.

Remark 1.3.11 (Blood isotropy justification). Blood is often modeled as an isotropic fluid since its microstructure (RBCs, WBCs, platelets) are suspended in plasma and distributed uniformly in all directions at macroscopic scales. This uniform distribution leads to isotropic mechanical properties, meaning blood's response to deformation is independent of direction. [[5], sec. 3.1] (Check source)

Definition 1.3.12 (Newtonian, isotropic constitutive law)**.** For a Newtonian, isotropic fluid the Cauchy stress is

$$\boldsymbol{T} \;=\; -p\,\mathrm{I} + 2\,\eta\,\boldsymbol{D}(\boldsymbol{u}) + \lambda\,\mathrm{div}(\boldsymbol{u})\,\mathrm{I},$$

where the bulk viscosity $\lambda \in \mathbb{R}^+$ is a material parameter quantifying the fluid's resistance to uniform compression.

So newtonian isotropic fluids at rest (quiescent state) sustains only hydrostatic stress:

$$\implies \boldsymbol{T} \;=\; -\,p\,\mathrm{I} \quad \text{when } \boldsymbol{u} \equiv \mathbf{0}.$$

Consequently, the constitutive law for newtonian fluids 1.3.12 simplifies under incompressibity assumption, because then $\operatorname{div}(\boldsymbol{u}) \;=\; 0$ in Ω_B (refer to 1.3.4).

Definition 1.3.13 (Incompressible stress tensor)**.** The Cauchy stress 1.3.12 simplifies to

$$\boldsymbol{T} \;=\; -\,p\,\mathrm{I} + 2\,\eta\,\boldsymbol{D}(\boldsymbol{u}).$$

Remark 1.3.14 (Dynamic vs. Kinematic Viscosity). In our model assumptions, *dynamic viscosity* $\eta \in \mathbb{R}^+$ and *kinematic viscosity* $\mu \in \mathbb{R}^+$ relate as

$$\mu \;:=\; \frac{\eta}{\rho} \;=\; \frac{\eta}{\rho_0} \;\in\; \mathbb{R}^+.$$

Here η quantifies the internal resistance of blood to shear deformation, i.e., $\eta \;:=\; \dfrac{\tau}{\dot{\gamma}}$, with units $\left[\, Pa \cdot s \,\right]$. Moreover μ adjusts η by the density ρ, capturing the viscous diffusion of momentum per unit mass, with units $\left[\, \frac{cm^2}{s} \,\right]$. Intuitively, η measures how "thick" or "sticky" the fluid is, while μ measures how quickly momentum diffuses through the fluid due to viscosity.

Remark 1.3.15 (Newtonian Blood Justification). When diameter d and hematocrit effects are needed, one may use a Non-Newtonian model with relative viscosity $\eta_r(H, d)$ that scales an absolute baseline η:

$$\eta_{\text{eff}} \;:=\; \eta_r(H,d)\,\eta \quad \text{(effective viscosity)}$$

An empirical fit from [6]

$$\eta_r \;:=\; 1 + (\eta_{0.45} - 1)\,\frac{(1-H)^C - 1}{(1-0.45)^C - 1} \text{ s.t. } \begin{cases} \eta_{0.45} = 6\,e^{-0.085\,d} + 3.2 - 2.44\,e^{-0.06\,d^{0.645}}, \\ C = \left(0.8 + e^{-0.075\,d}\right)\left(\dfrac{1}{1+10^{-11}\,d^{12}} - 1\right) + \dfrac{1}{1+10^{-11}\,d^{12}}, \end{cases}$$

where $d \;:=\; 2R/(1.0\mu m)$ is the (scaled) vessel diameter. In large vessels, η_r is often constant, justifying the Newtonian assumption. [[5], sec. 3.1]

When modeling non-Newtonian effects (when $\eta \neq$ constant), the kinematic viscosity $\mu(\cdot)$ is often chosen by

Carreau model [4]

$$2\,\mu(|\boldsymbol{D}|^2) = \eta_\infty + (\eta_0 - \eta_\infty)\cdot\big(1 + \kappa|\boldsymbol{D}|^2\big).$$

Where η_0 and η_∞ are chosen to be the viscosity for very small and very large shear rates, resp., and $\kappa \in \mathbb{R}^+$ and $n \in (-0.5, 0)$ are model parameters. According to [[5], pg. 38], we often set

$$\eta_0 = 65.7\cdot 10^{-3}\ Pa\cdot s,\ \eta_\infty = 4.45\cdot 10^{-3}\ Pa\cdot s, \kappa = 212.2\ s^2,\ \text{ and } n = -0.325$$

In the Newtonian case, we choose $\eta = \eta_\infty$ which allows us to determine μ as $\mu(|\boldsymbol{D}|^2) = \eta$.

1.4 Navier-Stokes

When coupling our momentum balance equation with the divergence-free condition of $\boldsymbol{u}$, we obtain the Navier-Stokes (NS) equations. We present several equivalent forms of the NS equations below. First, we write the NS system in conservative form.

Definition 1.4.1 (Conservative-Momentum Balance Form)**.**

$$\begin{cases} \partial_t(\rho\boldsymbol{u}) \ + \ (\rho\boldsymbol{u}\cdot\nabla)\boldsymbol{u} \ = \ -\nabla p \ \ \mathbf{div}\big(2\,\eta\,\boldsymbol{D}(\boldsymbol{u})\big) \ \ \rho\,\boldsymbol{f}, \\ \mathrm{div}(\boldsymbol{u}) \ = \ 0, \qquad \rho \ \equiv \ \rho_0 > 0 \text{ (constant)}. \end{cases}$$

Since $\rho \ \equiv \ \rho_0$ and $\eta \ \equiv \ \mu|\boldsymbol{D}|^2$, the advective form follows from 1.4.1.

Definition 1.4.2 (Generalized-Newtonian Navier-Stokes (NS))**.**

$$\begin{cases} \rho\big(\partial_t\boldsymbol{u} + (\boldsymbol{u}\cdot\nabla)\boldsymbol{u}\big) \ = \ -\nabla p \ + \ \mathbf{div}\Big(2\,\mu(|\boldsymbol{D}|^2)\,\boldsymbol{D}\Big) \ + \ \rho\,\boldsymbol{f} \\ \mathrm{div}(\boldsymbol{u}) = 0, \end{cases}$$

We divide ρ and obtain the kinematic-viscosity form from 1.4.2 as presented in [5], [3], and [4] (confirm).

Definition 1.4.3 (Kinematic-Viscosity Navier-Stokes (NS))**.**

$$\begin{cases} \partial_t\boldsymbol{u} + (\boldsymbol{u}\cdot\nabla)\boldsymbol{u} \ = \ -\frac{\nabla p}{\rho} \ + \ \mathbf{div}\Big(\frac{2}{\rho}\,\mu(|\boldsymbol{D}|^2)\,\boldsymbol{D}\Big) \ + \ \boldsymbol{f}, \\ \mathrm{div}(\boldsymbol{u}) = 0, \end{cases}$$

Finally, we write the NS system in operator form. (check arguments of F. Rewrite with Laplacian instead of divergence of stress tensor?)

Definition 1.4.4. We write Eq. 1.4.2 in standard form

$$\begin{cases} F\big(\partial_t \boldsymbol{u},\, \nabla \boldsymbol{u},\, \nabla p,\, \boldsymbol{u},\, p;\, \rho, \mu\big) \;=\; \boldsymbol{f}, \\ \operatorname{div}(\boldsymbol{u}) \;=\; 0, \end{cases}$$

where $F\big(\partial_t \boldsymbol{u},\, \nabla \boldsymbol{u},\, \nabla p,\, \boldsymbol{u},\, p;\, \rho, \mu\big) \;:=\; \partial_t \boldsymbol{u} \;+\; (\boldsymbol{u}\cdot\nabla)\boldsymbol{u} \;+\; \dfrac{\nabla p}{\rho} \;-\; \mathbf{div}\Big(\dfrac{2}{\rho}\,\mu\,(|\boldsymbol{D}|^2)\,\boldsymbol{D}\Big)$

Remark 1.4.5. The NS equations are a non-linear coupled system of PDEs. The first equation follows from the balance of linear momentum and it's terms are characterized as:

- The convective term $(\boldsymbol{u}\cdot\nabla)\boldsymbol{u} = \begin{bmatrix} \langle \boldsymbol{u},\, \nabla \boldsymbol{u}_1 \rangle \\ \langle \boldsymbol{u},\, \nabla \boldsymbol{u}_2 \rangle \\ \langle \boldsymbol{u},\, \nabla \boldsymbol{u}_3 \rangle \end{bmatrix}$ governs acceleration of fluid (non-linear).
- The diffusive term $\mathbf{div}\Big(2\,\mu(|\boldsymbol{D}|^2)\,\boldsymbol{D}\Big)$ describes the viscouselastic behavior (linear since μ is constant).

The second equation is the continuity equation, a consequence of the assumed fluid properties of blood that lead to the divergence-free condition on $\boldsymbol{u}$. The total system comprises of four equations in four unknowns: the three components of the velocity field $\boldsymbol{u}$ and the pressure field p.

If pressure p and the velocity $\boldsymbol{u}$ are given, the Cauchy stress $\boldsymbol{T}$ is computed from Eq. 1.3.13. It follows that the wall shear stress (WSS) at the vessel wall is:

$$\text{WSS} \;:=\; \langle \boldsymbol{t_{blood}},\, \boldsymbol{T}\,\hat{n}\rangle \quad : \quad \begin{cases} t_{blood} \text{ is tangent of a flow line through a cross-sectional area} \\ \hat{n} \text{ is outer normal of the cross-sectional area} \end{cases}$$

Forgoing the rigid-wall assumption allows us to model the relationship between the vessel wall and blood flow. Applicable models are referred to as fluid-structure interaction (FSI) models. discuss in a later section

1.5 Existence and Uniqueness of NS

Remark 1.5.1 (Global Regularity Problem for (NS)). *For any smooth, spatially localized initial data* $\mathbf{u}_0$*, does there exist a global smooth solution* $(\mathbf{u}, p)$ *to NS 1.4.2, when* $N = 3$*. Such question is one of the Millennium Prize Problems posed by the Clay Mathematics Institute in 2000, with a prize of one million dollars for a correct solution.*

Theorem 1.5.2 (Local Existence and Uniqueness)**.** *Given smooth, localized initial data* $\boldsymbol{u}_0$*, there exists a maximal time* $0 < T_* \leq \infty$ *for which a unique solution exists.*

If $T_* < \infty$, a **blow-up** occurs:

$$\sup_{x\in\mathbb{R}^3} |\mathbf{u}(t,x)| \to +\infty \quad \text{as} \quad t \to T_*.$$

Otherwise, if $T_* = \infty$, then $|\boldsymbol{u}| \to 0$ as $t \to \infty$. Numerical evidence suggests global regularity holds in most practical cases, but turbulent behavior can emerge for large initial data.

Heuristic Considerations and Energy Balance

Starting from the incompressibility condition:

$$\begin{aligned}
&\operatorname{div}(\boldsymbol{u}) = 0 \\
&\iff \quad \rho \text{ is constant in } \Omega(t) \\
&\iff \quad \text{chain rule applies to } \mathbf{div}\big(\frac{2}{\rho}\mu(|\boldsymbol{D}|^2)\boldsymbol{D}\big) \\
\implies &\mathbf{div}\big(\frac{2}{\rho}\mu(|\boldsymbol{D}|^2)\boldsymbol{D}\big) = \nabla \cdot \big(\frac{2}{\rho}\mu(|\boldsymbol{D}|^2)\boldsymbol{D}\big) \\
&= \langle \frac{2}{\rho}\mu(|\boldsymbol{D}|^2)\boldsymbol{D}, \nabla \rangle \\
&= \frac{2}{\rho}\langle \mu(|\boldsymbol{D}|^2)\boldsymbol{D}, \nabla \rangle \\
&= \frac{2}{\rho}\nabla \cdot \big(\mu(|\boldsymbol{D}|^2)\boldsymbol{D}\big) \\
&\therefore \quad \frac{2}{\rho}\,\mathbf{div}\big(\mu(|\boldsymbol{D}|^2)\boldsymbol{D}\big) = 0.
\end{aligned}$$

This vanishes if μ is constant (Newtonian fluid) and ρ is constant (incompressibility). So the diffusive term becomes:

$$\frac{2\eta}{\rho}\Delta \boldsymbol{u}, \quad \text{with } \eta = \mu\rho.$$

We heuristically compare dominant terms:

show simplification of diffusive term to laplacian

1. If $\eta\Delta \boldsymbol{u} \gg (\boldsymbol{u} \cdot \nabla)\boldsymbol{u}$, viscous dissipation dominates $\Rightarrow$ smooth, regular behavior.
2. If $(\boldsymbol{u} \cdot \nabla)\boldsymbol{u} \gg \eta\Delta \boldsymbol{u}$, nonlinearity dominates $\Rightarrow$ turbulence, potential blow-up.

We construct rigorous energy estimates in Section **??**.

1.5.1 NS in Cylindrical Coordinates

The relationship between cartesian and cylidrical coordinates is

$$(x,\ y,\ z) \ \mapsto (r\sin(\theta),\ r\cos(\theta),\ z), \quad r = \sqrt{x^2 + y^2}.$$

Let (r, θ, z) denote cylindrical coordinates on $\mathbb{R}^3$ with orthonormal basis $(\epsilon_r, \epsilon_\theta, \epsilon_z)$, and write the velocity

as

$$\begin{aligned}\boldsymbol{u}(t,r,\theta,z) \;&\equiv\; u_r(t,r,\theta,z)\,\epsilon_r \;+\; u_\theta(t,r,\theta,z)\,\epsilon_\theta \;+\; u_z(t,r,\theta,z)\,\epsilon_z.\\ &=\; u_r\,\epsilon_r \;+\; u_\theta\,\epsilon_\theta \;+\; u_z\,\epsilon_z\end{aligned}$$

where $u_r, u_\theta, u_z : \Omega_B \to \mathbb{R}$ are the cylindrical velocity components in the radial, azimuthal, and axial directions respectively. Then the kinematic-viscosity form of NS 1.4.3 in cylindrical coordinates involves the following differential operators:

$$\begin{aligned}(\boldsymbol{u}\cdot\nabla) \;&=\; u_r\,\partial_r \;+\; \frac{u_\theta}{r}\,\partial_\theta \;+\; u_z\,\partial_z,\\ \nabla p \;&=\; \partial_r p\,\epsilon_r \;+\; \frac{1}{r}\,\partial_\theta p\,\epsilon_\theta \;+\; \partial_z p\,\epsilon_z,\\ \operatorname{div}(\boldsymbol{u}) \;&=\; \frac{1}{r}\,\partial_r(ru_r) \;+\; \frac{1}{r}\,\partial_\theta u_\theta \;+\; \partial_z u_z.\end{aligned}$$

The components of the rate-of-strain tensor $\boldsymbol{D} = \frac{1}{2}\big(\nabla\boldsymbol{u} + (\nabla\boldsymbol{u})^\top\big)$ with respect to $(\epsilon_r, \epsilon_\theta, \epsilon_z)$:

$$\begin{aligned}&D_{rr} = \partial_r u_r, && D_{\theta\theta} = \frac{1}{r}\,\partial_\theta u_\theta + \frac{u_r}{r}, && D_{zz} = \partial_z u_z,\\ &D_{r\theta} = \frac{1}{2}\Big(\partial_r u_\theta - \frac{u_\theta}{r} + \frac{1}{r}\,\partial_\theta u_r\Big), && D_{rz} = \frac{1}{2}\big(\partial_r u_z + \partial_z u_r\big), && D_{\theta z} = \frac{1}{2}\Big(\frac{1}{r}\,\partial_\theta u_z + \partial_z u_\theta\Big)\end{aligned} \qquad .$$

The viscous (extra) stress is $\boldsymbol{\tau} = 2\,\mu(|\boldsymbol{D}|^2)\,\boldsymbol{D}$, so

$$\tau_{ij} = 2\,\mu(|\boldsymbol{D}|^2)\,D_{ij}, \qquad i,j \in \{r,\theta,z\}.$$

Writing $\boldsymbol{f} = f_r\,\epsilon_r + f_\theta\,\epsilon_\theta + f_z\,\epsilon_z$, the three components of the momentum equation are

$$\begin{aligned}\text{(radial)}\quad &\partial_t u_r + u_r\partial_r u_r + \frac{u_\theta}{r}\partial_\theta u_r + u_z\partial_z u_r - \frac{u_\theta^2}{r}\\ &\qquad =\; -\frac{1}{\rho}\,\partial_r p + \frac{1}{\rho}\Big[\frac{1}{r}\partial_r(r\tau_{rr}) + \frac{1}{r}\partial_\theta\tau_{r\theta} + \partial_z\tau_{rz} - \frac{1}{r}\tau_{\theta\theta}\Big] + f_r,\\ \text{(azimuthal)}\quad &\partial_t u_\theta + u_r\partial_r u_\theta + \frac{u_\theta}{r}\partial_\theta u_\theta + u_z\partial_z u_\theta + \frac{u_r u_\theta}{r}\\ &\qquad =\; -\frac{1}{\rho r}\,\partial_\theta p + \frac{1}{\rho}\Big[\frac{1}{r}\partial_r(r\tau_{r\theta}) + \frac{1}{r}\partial_\theta\tau_{\theta\theta} + \partial_z\tau_{\theta z} + \frac{1}{r}\tau_{r\theta}\Big] + f_\theta,\\ \text{(axial)}\quad &\partial_t u_z + u_r\partial_r u_z + \frac{u_\theta}{r}\partial_\theta u_z + u_z\partial_z u_z\\ &\qquad =\; -\frac{1}{\rho}\,\partial_z p + \frac{1}{\rho}\Big[\frac{1}{r}\partial_r(r\tau_{rz}) + \frac{1}{r}\partial_\theta\tau_{\theta z} + \partial_z\tau_{zz}\Big] + f_z.\end{aligned}$$

The incompressibility condition in cylindrical coordinates is

$$\frac{1}{r}\,\partial_r(ru_r) \;+\; \frac{1}{r}\,\partial_\theta u_\theta \;+\; \partial_z u_z \;=\; 0.$$

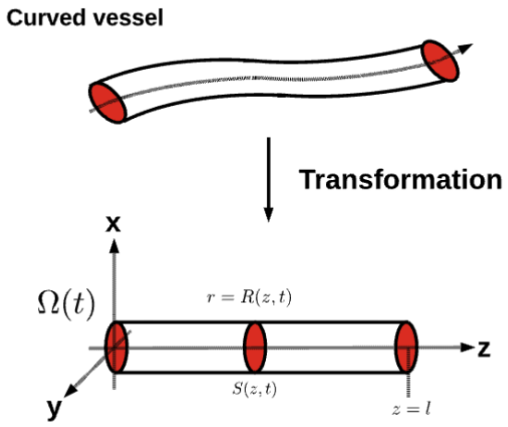

Figure 1: From [5] [Fig. 3.2, pg. 37]: A compliant vessel with time-dependent radius $R(z,t)$ along the axial position z. Since $\partial\Omega_B \in C^1$, the normal vector $\hat{n}$ is well-defined a.e. on the boundary. We assume such transformation is possible for blood vessels in our model.

Assume a vessel of length ℓ is aligned with the z-axis whose cross-section is circular with radius $R(z,t)$ at axial position z and time t. Our fluid domain becomes

$$\Omega(t) \;=\; \{(r,\ \theta\ , z) \in \mathbb{R}^3 \;:\; r \in [0, R(z,t)],\ \theta \in [0, 2\pi),\ z \in [0, \ell)\}$$

where $R(z,t)$ is the vessel radius at axial position z and time t.

WIP: continue from here...

2 Modeling Flow in a Single Vessel

We seek solution $\boldsymbol{u}$ to initial and boundary value problems of Eq. 1.4.3. Let $\boldsymbol{u}_0 : \Omega_B(0) \to \mathbb{R}^N,\ \boldsymbol{x} \mapsto \boldsymbol{u}_0(\boldsymbol{x})$ such that $\mathrm{div}(\boldsymbol{u}_0) = 0$ in $\Omega_B(0)$. Then the initial condition is given by the initial *velocity profile* $\boldsymbol{u}_0$

$$\boldsymbol{u}(\boldsymbol{x}, 0) \;:=\; \boldsymbol{u}_0(\boldsymbol{x}) \quad \forall \boldsymbol{x} \in \Omega_B(0).$$

In practice, $\boldsymbol{u}_0(\boldsymbol{x})$ may be prescribed or determined from sensor data. For the boundary conditions, we consider the following:

Definition 2.0.1 (Inlet Boundary Condition)**.** Let $\boldsymbol{u}_0(\boldsymbol{x}) : S_1(0) \to \mathbb{R}^N$ be a prescribed velocity profile at the inlet boundary $S_1(0)$.

Definition 2.0.2 (Outlet Boundary Condition)**.** Let $p_{out}(t) : I_T \to \mathbb{R}^+$ be a prescribed pressure profile at the outlet boundary $S_2(0)$.

Above definitions 2.0.1 and 2.0.2 are a particular choice of suitable boundary conditions for solving Eq. 1.4.3.

Other choices of boundary conditions are possible, e.g., prescribing periodic velocity profiles at the inlet and outlet boundaries of $\Omega_B(t)$; e.g., for modeling blood flow in a closed loop.

We start our discussion with 1D and 0D models, reducing the d.o.f. in the NS system 1.4.2 by imposing further simplifying assumptions. Such dimension reduced models compute average pressures and velocities after a relatively short simulation time, yeilding uniform distributions of WSS on the vessel wall $\Omega_W(t)$ at each time $t \in I_T$. Then we disscuss 2D models, which resolve velocity profiles in a vessel's cross-sectional plane, thus capturing WSS variations along the vessel wall. Finally, we discuss 3D models, which resolve full velocity profiles in a vessel, thus capturing complex flow patterns such as recirculation zones and vorticess.

2.1 0D Models

A simple reduction of the kinematic viscosity NS equations 1.4.3 is obtained by averaging pressure and velocity over a vessel's cross-sectional area. This yields a lumped-parameter model, often called a 0D model, where pressure and velocity are functions of time only. Herein 2.1, we discuss several 0D models, starting with the Windkessel model, a simple RC circuit analog for blood flow in large vessels. Then, we discuss more complex 0D models that include inertial effects and nonlinearities.

2.2 1D Models

The 1D model reduces the spatial dimension of the NS system by assuming axial symmetry of the vessel and averaging pressure and velocity over cross-sectional areas orthogonal to the vessel centerline. One may start by introducing a rigid-vessel assumption, which leads to a no slip condition that $\boldsymbol{u}\big|_{\partial\Omega_B(t)} = \mathbf{0}$. Instead we seek to model the link between blood flow and the deformation of the vessel wall. We begin our derivation of Dimension-Reduced models by assuming the following transformation exists of our fluid domain boundary $\Omega(t)$ to a simplified geometry.

We consider the fluid dynamics of the following fluid element contained in a portion of the lumen $\Omega(t)$ Let $S_1(t),\ S_2(t)$ be the time-dependent shaded boundaries at $z = z_1$ and $z = z_2$ s.t. $0 < z_1 < z_2 < \ell$. Let $V(t)$ be the fluid element of blood. The boundary of the fluid element is $\partial V(t) = S_1(t) \cup S_2(t) \cup \partial V(t)_w$ such that $\partial V(t)_w$ is the vessel wall in contact with the fluid element. According to the Reynold's transport theorem for scalar feild $\phi \in L^1(\Omega(t))$

$$\begin{aligned}\frac{d}{dt}\int_{V(t)} \phi(t,\boldsymbol{x})\,d\boldsymbol{x} &= \int_{V(t)} \partial_t\phi(t,\boldsymbol{x}) + \langle \nabla,\ \phi(t,\boldsymbol{x})\widehat{\boldsymbol{u_b}}(t,\boldsymbol{x})\rangle\,d\boldsymbol{x} \\ &= \int_{V(t)} \partial_t\phi(t,\boldsymbol{x})\,d\boldsymbol{x} \ + \ \int_{\partial V(t)_w} \langle \widehat{\boldsymbol{u_b}}(t,\boldsymbol{x}),\ \hat{\boldsymbol{n}}\rangle\phi(t,\boldsymbol{x})\,dS_{\boldsymbol{x}},\end{aligned}$$

where $\widehat{\boldsymbol{u_b}}$ is the velocity feild on the boundary $\partial V(t)$ (Pf. see wiki). If we assume the normal component of $\widehat{\boldsymbol{u_b}} = \mathbf{0}$ near the inlet and outlet boundaries S_1 and S_2 (resp.) of Ω, then the motion of the vessel wall

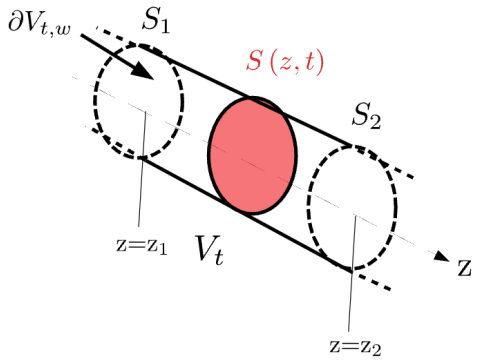

Fig. 3.3 Notation describing the different parts of the vessel portion

‘’

Figure 2: From [5] [Fig. 3.3, pg. XX]

is coupled to the blood flow through the fluid element $V(t)$. The velocity $\widehat{\boldsymbol{u_b}}$ is equivalent to the velocity of the vessel wall $\partial\Omega(t)$ in contact with the boundary element ∂_t. I.e., the vessel wall velocity $\boldsymbol{u_w} = \widehat{\boldsymbol{u_b}}$. Now let $\boldsymbol{w} = \boldsymbol{u_w} - \boldsymbol{u}$ be the relative velocity of the vessel wall w.r.t. the velocity $\boldsymbol{u} = (u_1, u_2, u_3)^\top$ of the blood element $V(t)$. Then it follows that

$$\begin{aligned}\int_{\partial_t} (\widehat{\boldsymbol{u_b}} \cdot \hat{\boldsymbol{n}})\phi \; dS_{\boldsymbol{x}} \;&=\; \int_{\partial_t} (\boldsymbol{u_w} \cdot \hat{\boldsymbol{n}})\phi \; dS_{\boldsymbol{x}} \\ &= \int_{\partial_t} (\boldsymbol{w} \cdot \hat{\boldsymbol{n}})\phi \; dS_{\boldsymbol{x}} \;+\; \int_{\partial_t} (\boldsymbol{u} \cdot \hat{\boldsymbol{n}})\phi \; dS_{\boldsymbol{x}}\end{aligned}$$

Let $\bar{\phi}$ denote the average value of ϕ defined over a surface S

$$\bar{\phi} \;:=\; \frac{1}{A} \int_{S(z,t)} \phi \; dS_{\boldsymbol{x}} \quad : \quad A(z,t) \;:=\; \int_{S(z,t)} dS_{\boldsymbol{x}}$$

Now we may rewrite the volume integral in the LHS of RT theorem

$$\int_{V(t)} \phi dV \;=\; \int_{z_1}^{z_2} \int_{S(z,t)} \phi \; dS_{\boldsymbol{x}} \, dz \;=\; \int_{z_1}^{z_2} A \cdot \bar{\phi} \, dz$$

where $z_1 < z_2$ are fixed z-coordinates for S_1 and S_2. Then we differentiate the integrands in the above equation w.r.t. t

$$\int_{V(t)} \frac{\partial \phi}{\partial t} dV \;=\; \int_{z_1}^{z_2} \frac{\partial}{\partial t} \left[A \cdot \bar{\phi} \right] dz,$$

and we've rewritten the first term in the RHS of the reynolds system. The surface integral in the RHS may be written as

$$\int_{\partial_t} (\widehat{\boldsymbol{u_b}} \cdot \hat{\boldsymbol{n}})\phi \, dS_{\boldsymbol{x}} = \int_{\partial_t} (\widehat{\boldsymbol{u_b}} \cdot \hat{\boldsymbol{n}})\phi \, dS_{\boldsymbol{x}} \ldots.$$

With a little more work, one may obtain:

cleanup, ref. pg. 43

Definition 2.2.1. The 1D Reynolds Transport theorem for both compressible and incompressible fluids:

$$\frac{\partial}{\partial t}\left(A\bar{\phi}\right) + \frac{\partial}{\partial z}\left(A(\overline{\phi \cdot u_3})\right) = \int_S \left(\frac{\partial \phi}{\partial t} + \nabla \cdot (\phi \boldsymbol{u})\right) dS_{\boldsymbol{x}} + \int_{\partial S} \phi \boldsymbol{w} \cdot \hat{\boldsymbol{n}}\, d\gamma$$

Remark 2.2.2. By taking $\phi = \rho$ in 2.2.1, mass conservation follows directly. Also, by our assumption that blood is incompressible, we have $\begin{cases} \operatorname{div}(\boldsymbol{u}) = 0 \\ \rho = \text{const.} \end{cases}$ and we simplify 2.2.1 as

$$\frac{\partial A}{\partial t} + \frac{\partial}{\partial z}\left(A(\overline{u_3})\right) = \int_{\partial S} \boldsymbol{w} \cdot \hat{\boldsymbol{n}}\, d\gamma$$

The RHS term above describing the transport process across the vessel wall.

complete, pg. 45

Remark 2.2.3. By taking $f = u_3$ in 2.2.1, momentum conservation follows directly. Also, by our assumption that blood is incompressible, we simplify 2.2.1 as

$$\frac{\partial}{\partial t}\left(Au_3\right) + \frac{\partial}{\partial z}\left(A(\overline{u_3^2})\right) = \int_S \left(\frac{\partial u_3}{\partial t} + \nabla u_3 \cdot \boldsymbol{u}\right) dS_{\boldsymbol{x}} + \int_{\partial S} u_3 \boldsymbol{w} \cdot \hat{\boldsymbol{n}}\, d\gamma$$

The RHS term above describing the transport process across the vessel wall.

2.3 2D Models

2.4 3D Models

3 Lerning Arterial Flow via PINNs

As disscussed in Sec. 2, traditional numerical methods for solving the NS equations, such as finite difference methods (FDM), finite element methods (FEM), and finite volume methods (FVM), require discretizing the spatial domain $\Omega_B(t)$ into a mesh or grid. An alternative approach leverages modern machine learning (ML) techniques, particularly deep neural networks (DNNs), to learn solution representations to the NS equations. Physics-informed neural networks (PINNs) are the first class of DNNs we discuss for learning arterial flows. Then we discuss Deep-Riesz DNNs, a recent class of DNNs for learning weak solution representations to PDEs.

A DNNs are universal function approximators, able to learn arbitrary nonlinear mappings between finite-dimensional spaces. This property is formalized in the following theorem.

Theorem 3.0.1 (Universal Approximation Theorem of Nonlinear Operators)**.**

TW-Bauer continuity conditions...

3.1 Pysics-Informed Neural Networks

Machine learning techniques for learning solutions to initial-boundary value problems were first proposed by Lagaris et al. **??** in 1998. Since then, a variety of neural network architectures and training strategies have been proposed for learning solutions to PDEs. In this section, we introduce physics-informed neural networks (PINNs), one of the most widely used methods for learning forward and inverse problems.

PINNs were introduced by Raissi et al. (**??**, 2019) as a unified framework to tackle two distinct but related problems, namely,

1. Data driven solutions: inference problems for both forward and inverse initial-boundary value problems.
2. Data driven discovery of PDEs: discovering the parameters and structure of of the underlying differential operator governing the observed data.

In both cases, numerical expeirments where conducted using a feed-forward DNN (FNN) architecture with hyperbolic tangent activation function $\boldsymbol{\sigma}$ on classical problems in mathematical physics.

Definition 3.1.1. An L-layer (or $L-1$ hidden layer) **feed-forward neural network (FNN)** is defined recursively as

$$\begin{aligned}
\text{input layer: } \boldsymbol{N_0}(\boldsymbol{x}) &= \boldsymbol{x} \in \mathbb{R}^{d_{in}} \\
\text{hidden layer: } \boldsymbol{N_l}(\boldsymbol{x}) &= \boldsymbol{\sigma}\big(\boldsymbol{N_l}(\boldsymbol{x}) = \boldsymbol{W_l N_{l-1}}(\boldsymbol{x}) + \boldsymbol{b_l}\big) \in \mathbb{R}^{N_l},\ \forall l \in [L-1] \\
\text{output layer: } \boldsymbol{N_L}(\boldsymbol{x}) &= \boldsymbol{W_L N_{L-1}}(\boldsymbol{x}) + \boldsymbol{b_L} \in \mathbb{R}^{d_{out}},
\end{aligned}$$

so that $N(\boldsymbol{x}) : \mathbb{R}^{d_{in}} \mapsto \mathbb{R}^{d_{out}}$ is the FNN, $\boldsymbol{W_l} \in \mathbb{R}^{N_l \times N_{l-1}}$ are the weight matrices, and $\boldsymbol{b_l} \in \mathbb{R}^{N_l}$ are the bias vectors. Here N_l is the number of neurons in the l-th layer, and the nonlinear activation function $\boldsymbol{\sigma} : \mathbb{R}^{N_l} \mapsto \mathbb{R}^{N_{l+1}}$ is applied component-wise.

Funamental to any ML task is to define a suitable loss function $\mathcal{L}_{\text{obj}}(\boldsymbol{\theta})$, where $\boldsymbol{\theta}$ is the vector of all weights and biases in the network to be optimized.

Now we can write $\boldsymbol{\theta} = \{\boldsymbol{W_l}, \boldsymbol{b_l}\}_\forall l \in [L]$, and we'll denote the L-layer FNN as $N(\boldsymbol{x}; \boldsymbol{\theta}) = N_L(\boldsymbol{x})$. The backward-propogation step maps $\boldsymbol{\theta} \mapsto \boldsymbol{\theta}^*$ by solving the optimization problem

$$\boldsymbol{\theta}^* = \text{argmin}_{\boldsymbol{\theta}}\, \mathcal{L}_{\text{obj}}(\boldsymbol{\theta}). \tag{3.1.1}$$

Remark 3.1.2. The backward progation step of training refers to solving (3.1.1), which is commonly acheived using the following optimization algorithms:

- For small-regime dense networks, we often prefer a Quasi-Newton (QN) method like L-BFGS, due to its fast convergence and ability to converge to second-order stationary points. Precisely, such methods

escape saddle points by approximating the inverse Hessian $\boldsymbol{H}_k$ of the loss function at each iteration k with gradient information; providing local second-order information at iterate θ_k. The advantage of a QN method is that it approximates Newton dynamics but doesn't suffer the computational cost of calculating the full Hessian, as in Newton's method. A practical QN implementation takes step $\boldsymbol{s}_k$ minimizing the quadratic model

$$\begin{cases} \min_{\boldsymbol{s}} \ \mathcal{L}_{\text{obj}}(\boldsymbol{\theta}_k) + \nabla \mathcal{L}_{\text{obj}}(\boldsymbol{\theta}_k)^T \boldsymbol{s} + \frac{1}{2} \boldsymbol{s}^T \boldsymbol{H}_k \boldsymbol{s} \\ \text{s.t.} \ \ \langle \boldsymbol{s}, \ \boldsymbol{s} \rangle \leq \Delta_k^2, \end{cases} \tag{3.1.2}$$

where Δ_k is the trust-region radius at iteration k. I.e., in practice QN methods naviagate the loss function landscape by solving a series of trust-region subproblems instead of a traditional line search to determine $\boldsymbol{\theta}^{k+1} = \boldsymbol{\theta}^k + \boldsymbol{s}$. See Ch. 3 **??** for more details.

L-BFGS has been observed to outperform first-order methods for PINN training **??**. Following, Azzam et. al present an embarrassingly parallel algorithm for computing Jacobian-vector products during gradient evaluation using forward-mode automatic differentiation. Namely, when computing $\nabla \mathcal{L}_{\text{obj}}(\boldsymbol{\theta}_k)$ it is possible to compute $\boldsymbol{J}(\boldsymbol{\theta}_k)\boldsymbol{d}$ for any vector $\boldsymbol{d}$ at $O(1)$ additional cost. Then since $\boldsymbol{J}(\boldsymbol{\theta}_k)\boldsymbol{d} = \nabla^2 \mathcal{L}_{\text{obj}}(\boldsymbol{\theta}_k)\boldsymbol{d}$, naturally, this leads to strategies for sampling column space of $\nabla^2 \mathcal{L}_{\text{obj}}(\boldsymbol{\theta}_k)$. But note the optimal step $\boldsymbol{s}$ is obtained from (3.1.2) as:

$$\boldsymbol{s}_k = -(\boldsymbol{H}_k + \lambda \mathbf{I})^{-1} \nabla \mathcal{L}_{\text{obj}}(\boldsymbol{\theta}_k),$$

for some $\lambda \geq 0$ chosen to satisfy the trust-region constraint. Thus, by computing $\boldsymbol{J}(\boldsymbol{\theta}_k)\boldsymbol{d}$ for various $\boldsymbol{d}$, one can form a low-rank approximation of $\nabla^2 \mathcal{L}_{\text{obj}}(\boldsymbol{\theta}_k)$, and use the Sherman-Morrison-Woodbury formula to efficiently compute $(\boldsymbol{H}_k + \lambda \mathbf{I})^{-1} \nabla \mathcal{L}_{\text{obj}}(\boldsymbol{\theta}_k)$. Various sampling strategies are explored and implemented in the Julia-based software package **??**, where *ForwardDiff.jl* [7] provides the forward-mode AD capabilities. Future work on integrating this approach into PINN training for smaller dense networks is promising. [1]

provide more details/links to other commonly used QN implementations, e.g., Optim.jl, XGBoost, SciPy, etc.

- In medium-sized networks or problems requiring moderate accuracy, second-order methods like Newton-CG are preferred due to their ability to converge rapidly to second-order stationary points. Here, the Newton step $\boldsymbol{s}_k$ at iteration k is computed by solving the linear system

$$\nabla^2 \mathcal{L}_{\text{obj}}(\boldsymbol{\theta}_k)\boldsymbol{s} = -\nabla \mathcal{L}_{\text{obj}}(\boldsymbol{\theta}_k), \tag{3.1.3}$$

using the conjugate gradient (CG) method. Note, CG only requires Hessian-vector products $\nabla^2 \mathcal{L}_{\text{obj}}(\boldsymbol{\theta}_k)\boldsymbol{d}$,

which can be computed efficiently using Pearlmutter's method **??**. This allows Newton-CG to scale to larger problems than traditional Newton's method, which requires forming and storing the full Hessian matrix.

- For larger networks or problems with lower accuracy requirements, first-order methods like Adam or SGD are preferred due to their scalability resulting from low per-iteration computational cost. Note, such methods follow the dynamics of gradient flow, and consequently converge to first-order stationary points. However, there is research to suggest that convergence to saddle points is avoided in high-dimensional settings due to the abundance of negative curvature directions around such points **??**.

provide details/links to commonly used first-order optimizers, e.g., Flux.jl, PyTorch, TensorFlow, etc.
Confirm first order methods utilize reverse-mode AD?

3.2 PINNs Vs. FEM

	PINN	**FEM**
Basis function	NN(non-linear)	Piecewise polynomial (linear)
Parameters	Weights & biases	Point values
Training points	Scattered points (mesh-free)	Mesh Points
PDE embedding	Loss function	Algebraic System
Parameter Solver	Gradient-Based Optimizer	Linear Solve
Errors	$\epsilon_{app}, \epsilon_{gen}, \epsilon_{opt}$	Quadrature errors
Error bounds	Unknown	Partially Known

4 Appendix

Bibliography

References

[1] Joy Azzam et al. *QN Optimization with Hessian Sample*. 2022. arXiv: 2201.02608 [math.OC].

[2] Francois Derimay, Gerard Finet, and Gilles Rioufol. "Coronary Artery Stenosis Prediction Does Not Mean Coronary Artery Stenosis Obstruction". In: *European Heart Journal* (2021). DOI: 10.1093/eurheartj/ehab332. URL: https://watermark.silverchair.com/ehab332.pdf.

[3] Luca Formaggia and Alfio Quarteroni. *Mathematical Modeling and Numerical Simulation of the Cardiovascular System*. 2002.

[4] Giovanni P. Galdi et al. *Hemodynamical Flows: Modeling, Analysis and Simulation*. Birkhäuser Basel, 2008. DOI: https://doi.org/10.1007/978-3-7643-7806-6.

[5] Tobias Köppl and Rainer Helmig. *Dimension Reduced Modeling of Blood Flow in Large Arteries. An Introduction for Master Students and First Year Doctoral Students*. Springer Nature Switzerland, 2023.

[6] Gaehtgens P Pries AR Neuhaus D. "Blood viscosity in tube flow: dependence on diameter and hematocrit". In: *Am J Physiol.* (6 Pt 2).263 (1992). DOI: 10.1152/ajpheart.1992.263.6.H1770.

[7] J. Revels, M. Lubin, and T. Papamarkou. "Forward-Mode Automatic Differentiation in Julia". In: *arXiv:1607.07892 [cs.MS]* (2016). URL: https://arxiv.org/abs/1607.07892.

Code Listings

Code listings

Code 1: Algorithm 16.5

```
1        function foo()
2            println("Hello World)
3        end
```